Research Square

Preprints are preliminary reports that have not undergone peer review.
They should not be considered conclusive, used to inform clinical practice,
or referenced by the media as validated information.

A novel approach for significantly increasing cassava resistant starch (RS 3) yields by using mechanical activation combined with enzymatic hydrolysis

Zexiong Huang
Guangxi University
Tianyi Guo
Guangxi University
Xiaohua Huang
Guangxi University
Chen Liang
Guangxi University
Mingyu Chen
Guangxi state farm
Yanjuan Zhang
Guangxi University
Zuqiang Huang
Guangxi University
Huayu Hu
Guangxi University
Tao Gan
gant@gxu.edu.cn

Guangxi University

Research Article

Keywords: Resistant starch, Low-GI food, In vitro starch digestibility

Posted Date: April 24th, 2026

DOI: https://doi.org/10.21203/rs.3.rs-9241783/v1

License: This work is licensed under a Creative Commons Attribution 4.0 International License.
Read Full License

Additional Declarations: No competing interests reported.

Abstract

Foods containing resistant starch (RS) have the potential to regulate blood glucose levels, but the preparation of high-amylopectin starch with high RS_3 type resistant starch content is still challenging. Herein, cassava resistant starch (RS_3) was prepared by mechanical activation (MA) combined with enzymatic hydrolysis using high-amylopectin cassava starch as the raw material. The RS_3 content in the starch treated with MA and enzymatic hydrolysis (EMS) was 23.6%, while the RS_3 contents in the starch treated with only enzymatic hydrolysis (ES) and only MA (MS) were 13.6% and 9.9%, respectively. The MA treatment effectively disrupted the crystalline regions of starch, accelerating the enzymatic hydrolysis efficiency of pullulanase, which could generate more short amylose chains suitable for retrogradation, leading to an increase in RS_3 content. Moreover, EMS was used to prepare biscuits, and their glycemic index (GI) was measured to be 53.3 via *in vitro* digestion experiments, which met the criteria of low-GI foods, demonstrating the potential of EMS to regulate blood glucose. This study provides a new method for producing RS_3 and functional low-GI foods from high-amylopectin starch.

Introduction

According to the data of the World Health Organization, approximately 422 million people worldwide suffer from diabetes, and 1.5 million people die directly from diabetes each year. The glycemic index (GI) is used to assess the changes in blood glucose levels following food intake [1]. Consuming low-GI foods such as pasta and chickpeas can help regulate blood glucose and insulin functions in diabetic patients [2–4]. Resistant starch (RS) can provide satiety while also regulating blood sugar levels, the higher the RS content, the lower the GI of the prepared food [5–7]. Furthermore, RS can also reduce the risk of obesity, gastrointestinal diseases, and hypertension [7, 8]. RS can be categorized into five types: RS_1 (physically embedded starch), RS_2 (raw starch granules), RS_3 (retrograded starch), RS_4 (chemically modified starch), and RS_5 (starch-lipid complexes) [9, 10]. However, the current research on producing starch with high RS_3 content from high-amylopectin starch is still limited. Developing a simple and industrially feasible method for producing high-content RS_3 type starch from high-amylopectin starch is highly desired.

Previous researches have shown that RS_3 is primarily formed through the short-term gelatinization and crystallization of amylose, along with the long-term rearrangement of amylopectin into a dense and resistant structure [19–21]. Currently, RS_3 can be produced through various methods, including chemical modification, starch retrogradation, enzymatic hydrolysis, extrusion, and mechanical activation (MA) [11–16]. Due to growing consumer interest in the natural and organic foods for the health and environmental reasons, RS_3 formed through physical or enzymatic pretreatment, followed by starch retrogradation, appears to be especially appealing [17, 18]. Debranching enzyme treatment is an effective method to cleave the α-1,6-glycosidic bonds at amylopectin branching points, thereby increasing the amylose content and rearranging the structure to form RS_3 with a dense structure [22].

For instance, pullulanase treatment of pearl millet starch could increase the RS_3 content from 43.67% to 52.24% after 72 h of retrogradation [23]. However, enzymatic treatment is more suitable for high-amylose starch than for high-amylopectin starch, ascribing to that high-amylopectin starch consists of ordered crystalline and amorphous regions, which limit the enzyme access to cleave the α-1,6-glycosidic bonds, thus reducing enzymatic efficiency. Consequently, enzymatic treatment alone is insufficient for producing high-content RS_3 in high-amylopectin starch.

MA, as a simple and physical pretreatment method, can alter the structure and physicochemical properties of solid particles through friction, impact, and shearing forces, thus converting the mechanical energy into internal energy and enhancing reaction rates [24–26]. Our previous studies have found that the MA treatment could increase the amylose content of starch through partial cleavage of amylose and amylopectin chains to enhance interaction with water, solubility, and swelling power, which promoted the retrogradation for generating RS_3 [27–29]. However, short-term MA treatment can only slightly damage the outer structure of starch, while the internal crystalline structure of starch remains partially intact. Prolonging the MA treatment time, however, will lead to the production of excessively short amylose molecular chains, which is not conducive to starch retrogradation. Thus, MA treatment alone has limited effectiveness in increasing RS_3 content in high-amylopectin starch. For example, Liu et al. [30] reported that MA treatment increased the RS_3 content of cassava starch from 4% to approximately 13%. Therefore, using the method of MA process combined with enzymatic hydrolysis for the preparation of RS_3, part of the crystalline regions within the starch granules are disrupted by mechanical forces, allowing pullulanase to be evenly distributed and enter the crystalline regions to enhance enzymatic hydrolysis and accelerate starch debranching. Meanwhile, MA also breaks some amylopectin branches into amylose, thereby increasing the RS_3 content and improving the production efficiency.

Cassava is an important and cost-effective staple crop with the characteristics of high yield, drought and pest resistance, and low production cost [31, 32]. Cassava starch consists of approximately 80% of amylopectin, which is a high-amylopectin starch with high paste viscosity and elevated crystallinity, as well as stability against shearing and freezing [33]. In this work, RS_3-enriched cassava starch was prepared by a method of MA combined with enzymatic hydrolysis using high-amylopectin cassava starch as the raw material. The changes in starch structure were analyzed using DL-NMR, XRD, and SEM. RS_3-enriched starch was used to make low-GI biscuits, and the GI values were determined through *in vitro* digestion experiments. This study provides a new method for increasing RS_3 content in high-amylopectin cassava starch and developing corresponding low-GI foods.

Materials and methods

Materials

Cassava starch (food grade, HS1108140000, amylose content 18.32%) was supplied by Guangxi State Farms Mingyang Biochemical Group, INC (Nanning, China). Sodium hydroxide (NaOH, 99.0%), potassium hydroxide (KOH, 99.0%), acetic acid (99.0%), tris(hydroxymethyl)aminomethane (99.0%), maleic acid (99.0%), amyloglucosidase (100 u mg^{-1}), pullulanase (2 u mg^{-1}), α-amylase (3.5 u mg^{-1}), and pepsin (1: 3000) were procured from Macklin Biochemical Co., Ltd. (Shanghai, China). Peanut oil was purchased from a local Walmart store, and the Resistant Starch Assay Kit was obtained from Megazyme International Ireland Ltd. (Bray, Ireland).

Preparation of RS samples

Cassava starch was treated with MA and pullulanase, and the names of starch samples were assigned according to the treatment methods (native cassava starch was labeled as S). A 20% (w/w) starch solution was prepared by mixing S with pullulanase (20 u g^{-1}) and incubating in a shaker at 50°C for 6 h (the resulting starch sample was labeled as ES). Then, 100.0 g of ES was placed in a stainless steel chamber, with the addition of approximately 300 mL of grinding balls (diameter of 5 mm), and the ES was treated by MA with a speed of 300 rpm at 50°C for 30 min (the resulting starch sample was labeled as ES + M). Meanwhile, 100.0 g of S was treated by MA under identical conditions (the resulting starch sample was labeled as MS). MS was used to prepare a 20% (w/w) starch solution, and then was mixed with pullulanase (20 u g^{-1}) and incubated at 50°C for 6 h (the resulting starch sample was labeled as MS + E). Finally, a 20% (w/w) S solution with pullulanase (20 u g^{-1}) was placed in a stainless steel chamber with the addition of 300 mL of grinding balls, and the S was treated by MA with a speed of 300 rpm at 50°C for 6 h (the resulting starch sample was labeled as EMS). These starch samples were prepared into dough with a starch-to-water mass ratio of 5: 4, gelatinized at 100°C for 15 min, cooled to room temperature (20°C), and stored at 4°C for 7 d before drying, crushing, and storing for further analysis.**Characterization**

The RS content of all samples was measured using a Resistant Starch Assay Kit (Megazyme, Bray, Ireland) following the method recommended by the Association of Official Analytical Chemists (AOAC). XRD analysis was performed on a diffractometer (D/MAX2500V, Rigaku, Japan) using CuKα radiation (λ = 0.154 nm) at 40 kV and 30 mA, with a step size of 0.02° over a range of 5°—40°. Dried samples were mixed with dried KBr (1:100, w/w) in an agate mortar, pressed into tablets, and analyzed using a Nicolet IS 50 Fourier transform infrared spectrometer (Thermo Fisher, USA) within a wavenumber range of 500 to 4000 cm^{-1}. Sample blocks (1 × 1 × 1 cm) were wrapped in plastic wrap and placed in 25 mm diameter glass tubes. The transverse relaxation time was measured using an NMR analyzer (MicroMR20-025V-I, Niumag Co., Ltd., Suzhou, China). The thermal characteristics of each sample were determined using a differential scanning calorimeter (DSC, TAQ2000, Netzsch, Germany) over a temperature range of 20 to 120°C at a rate of 10°C min^{-1}. Dried cassava starch samples were mounted on aluminum stubs using double-sided adhesive tape and sputter-coated with gold. The samples were observed using an S-3000N scanning electron microscope (Hitachi, Japan).

Preparation of biscuits

The formula for making biscuits included 50.0 g of starch, 5.0 g of polydextrose, 6.0 g of peanut oil, 0.4 g of baking soda, and 16.0 g of water. Starch and baking soda were first mixed, followed by the addition of water to form a rough dough. Peanut oil was added to produce a smooth dough, which was then rolled into thin sheets, shaped with cookie cutters, and baked for 10 min at 190°C top heat and 170°C bottom heat. Baked biscuits were cooled to room temperature and stored in sealed containers.

Measurement of GI value of biscuits

Typically, 50 mg of biscuit samples were dispersed in 6 mL of 2M KOH and shaken at room temperature for 30 min. Then, 3 mL of 0.4 M sodium acetate buffer (pH = 4.75) and 60 μL of starch glucosidase were added to the suspension, which was incubated in a shaking water bath at 60°C for 45 min. The glucose content from starch hydrolysis was measured using the GOPOD assay, with a glucose conversion factor of 0.9 to calculate the total starch weight. Subsequently, 50 mg of biscuit samples and 10 mL of HCl-KCl buffer (pH = 1.5) were added to centrifuge tubes. With the addition of 0.2 mL of pepsin to each sample, they were incubated in a shaking water bath at 40°C for 1 h. After incubation, the volume was adjusted to 25 mL using Tris-Maleate buffer (pH = 6.9). To hydrolyze the starch, 5 mL of Tris-Maleate buffer containing 2.6 IU α-amylase was added to each sample, and then incubated in a shaking water bath at 37°C. At intervals of 0 to 180 min, 1.0 mL of sample was taken from each tube every 30 min, and these samples were heated at 100°C for 5 min to inactivate the enzyme. Then, 3 mL of 0.4 M sodium acetate buffer (pH = 4.75) and 60 μL of starch glucosidase were added, and the samples were incubated at 60°C in a shaking water bath for 45 min to complete the starch hydrolysis. The glucose content after hydrolysis was determined using the GOPOD assay kit [34].

The digestibility of starch was expressed as the percentage of total starch hydrolysis at different time points (30, 60, 90, 120, and 180 min) and was calculated as follows:

$$\text{Total starch hydrolysis (\%)} = \frac{(\text{digested glucose weight} \times 0.9)}{\text{total starch weight}} \times 100\% \quad (1)$$

The kinetics of *in vitro* starch digestion were calculated using the nonlinear model established by [34]. The first-order equation was:

$$C = C_{\infty}(1 - e^{-kt}) \quad (2)$$

where C is the percentage of hydrolyzed starch at time t (min), C_{∞} is the equilibrium percentage of hydrolyzed starch after 180 min, and k is the rate constant. The area under the hydrolysis curve (*AUC*) was calculated using the following formula:

$$AUC = C_{\infty}(t_f - t_o) - (C_{\infty}/k)[1 - \exp^{\{-k(tf-to)\}}] \quad (3)$$

where t_f is the final hydrolysis time (180 min), t_0 is the initial hydrolysis time (0 min), and k is the rate constant.

The hydrolysis index (*HI*) was obtained by dividing the *AUC* of the samples by the *AUC* of the reference (white bread). *HI* is a good predictor of the glycemic response and can be used to estimate the expected glycemic index (*GI*) using the following formula:

$$GI = 39.71 + 0.549 \times HI_{90} \quad (4)$$

where HI_{90} represents the hydrolysis index at 90 min.

Sensory evaluation of biscuits

A sensory evaluation was conducted by a panel of 10 trained members who assessed biscuit quality based on a quantitative descriptive analysis (QDA) [35]. Sensory parameters included color, appearance, flavor, fracturability, and inner structure. Each biscuit was observed on a white porcelain plate under natural light. After rinsing with warm water, each panelist chewed the biscuit sample to evaluate flavor and internal structure. Each parameter was rated on a scale of 0 to 10, and the overall score was calculated by averaging individual parameter scores to assess general acceptability.

Results and discussion

RS_3 content in starch and structural analyses

Figure S1 shows the effects of different treatments on RS_3 content. The RS_3 contents in the S, ES, and MS samples were determined to be 5.8, 13.6, and 9.9%, respectively. The high RS_3 content was attributed to the pullulanase treatment. Pullulanase could cleave the α-1,6-glycosidic bonds of starch, increasing the proportion of amylose and forming RS_3 with a compact structure. The increase in RS_3 content in the MS sample was also related to the increase in amylose, which might result from the mechanical disruption of amylopectin branches or the cleavage of long amylose chains in the native starch granules. The RS_3 content in the ES + M sample was 10.5%, which was lower than that of the ES sample. This might be due to the increase in amylose content after pullulanase treatment, which caused long amylose chains to broken into short chains during the MA process. Excessive short amylose chains were unfavorable for RS_3 formation, thus reducing the RS_3 content. The MS + E sample underwent MA treatment first, followed by pullulanase treatment. MA disrupted both amylopectin and amylose

molecules, and the mechanical force damaged the starch crystalline regions. This facilitated the entry of pullulanase into the crystalline regions, enhancing enzyme efficiency and further increasing the amylose content. Consequently, the RS_3 content in the MS + E sample was 16.8%, which was higher than those of MS and ES samples. For the EMS sample, the RS_3 content was 23.6%, attributed to that the MA treatment broke down part of the crystalline regions of starch, which promoted the uniform distribution of pullulanase to accelerate the debranching reaction. This caused the rupture of some amylopectin branches, forming amylose and significantly increasing the amylose content.

XRD analysis was used to investigate the changes in the crystalline structure of cassava starch treated by different methods, and the relative crystallinity (RC) was calculated based on the relative area of diffraction peaks, as shown in Fig. 1. Figure 1a shows the XRD patterns of the starch samples before retrogradation. All treated samples exhibited identical diffraction peak positions without any new peaks, indicating that MA and enzymatic hydrolysis did not alter the crystalline type of starch. The diffraction peaks appeared at 17°, 22°, and 23°, but their intensities decreased after treatment. The intensity of these peaks correlated with the crystallinity of starch, suggesting that the crystalline regions composed primarily of amylopectin were disrupted during treatment, resulting in a reduce in crystallinity [29]. This disruption facilitated the conversion of amylopectin to amylose by MA or enzymatic hydrolysis treatment, which likely promoted the formation of RS_3. The crystallinity of the starch samples subjected to a single treatment, either enzymatic hydrolysis (ES) or MA (MS), was 18.11% and 19.67%, respectively. For the sequentially treated starch samples (ES + M or MS + E), the crystallinity decreased further to 16.91% and 15.58%, respectively, suggesting that enzymatic hydrolysis and MA had a mutually enhancing effect to some extent. The starch sample treated by MA combined with enzymatic hydrolysis (EMS) exhibited the lowest crystallinity of 11.79%. This substantial decline was likely due to that the mechanical force during MA disrupted crystalline regions, allowing pullulanase to penetrate and hydrolyze amylopectin within these regions. Meanwhile, enzymatic hydrolysis further fragmented the amylopectin, resulting in a significant reduction in the crystallinity of the EMS samples. These findings support the conclusion that EMS had the highest amylose content, which contributed to facile retrogradation for increasing the formation of RS_3.

Figure 1b shows the XRD patterns of retrograded starch. The changes in crystallinity were primarily attributed to the recrystallization of amylose into RS_3 with dense structure. As the RS_3 content increasing, the crystallinity also rose. EMS exhibited the highest crystallinity of 26.69%, surpassing all other control samples. This result confirmed the synergistic effect between MA and enzymatic hydrolysis, which effectively converted amylopectin within crystalline regions into amylose, facilitating the production of high-content RS_3.

As shown in Fig. 1c, the FT-IR spectra of all samples exhibited the characteristic absorption peaks at 3436, 2931, and 1158 cm^{-1}, corresponding to O–H, $–CH_2$, and C–O–C groups, respectively. No new functional groups were observed, indicating that these treatments only altered the physical properties of the starch samples. Notably, the O–H stretching vibration peak at 3440 cm^{-1} was more pronounced in

EMS. Compared with other control samples, the absorption band within the range of 3600–3200 cm^{-1} was broader and deeper in EMS, suggesting the formation of additional hydrogen bonds. These bonds likely resulted from the interactions of short amylose chains with free hydroxyl vibrations and the complex interplay of intra- and intermolecular forces [41]. This phenomenon indicated a high RS_3 content in EMS. The intensity of the peak at 2930 cm^{-1} was also enhanced in EMS, reflecting changes in O–H and –CH vibration conformations, which were associated with the retrogradation process. These changes suggested the modifications in the starch structure, such as chain length, alignment, and crystallinity [42]. These findings, in combination with XRD results, demonstrated that the synergistic effects of MA and pullulanase more effectively converted amylopectin into amylose. During retrogradation, the short amylose chains in EMS formed the RS_3 with dense and highly crystalline structure through molecular interactions.

The RS, RC, and $IR_{1047/1022}$ (infrared absorbance ratio of 1047 cm^{-1}/1022 cm^{-1}) values of the starch samples treated by different methods were compared, as shown in Table 1. The absorbance at 1047 and 1022 cm^{-1} corresponded to the vibrational absorption of crystalline and amorphous regions in starch crystals, respectively [41, 42]. The $IR_{1047/1022}$ value is a quantitative index of starch, which reflects the degree of crystallinity and short-range ordered structure. An increase in $IR_{1047/1022}$ indicates a higher degree of starch recrystallization and vice versa. The RS, RC, and $IR_{1047/1022}$ values of the starch samples were increased with MA or enzymatic hydrolysis treatment. The RS, RC, and $IR_{1047/1022}$ values of MS were lower than those of MS + E, indicating that MA effectively disrupted the crystalline regions of starch. This disruption enhanced the enzymatic efficiency of pullulanase, producing more short amylose chains suitable for retrogradation. During retrogradation, these short amylose chains facilitated the formation of a dense crystalline structure, thereby increasing the RS_3 content.

Table 1
RS, RC, and IR of different treated starch samples.

Sample	RS (mg/100 mg)	RC (%)	$IR_{1047/1022}$
S	5.80	9.10	0.997
ES	13.60	19.89	1.014
ES + M	10.50	16.33	1.004
MS	9.90	15.86	1.003
MS + E	16.80	22.38	1.026
EMS	23.60	26.69	1.039

In contrast, ES exhibited higher RS, RC, and $IR_{1047/1022}$ values compared to ES + M, which suggested that enzymatic hydrolysis treatment first generated short amylose chains. However, subsequent MA further broke these short amylose chains into even shorter molecular fragments. Overly short amylose chains

were less capable of quickly forming the double-helix structure required for RS_3, leading to a decrease in RS_3 content. Among all treatments, EMS showed the highest RS, RC, and $IR_{1047/1022}$ values, which highlighted the pronounced synergistic effect of simultaneous MA and enzymatic hydrolysis treatment. When MA was conducted simultaneously with enzymatic hydrolysis, the crystalline structure of cassava starch granules was disrupted, which facilitated enzyme access and promoted the cleavage of branch points to generate linear chains. In addition, the friction and shear forces associated with MA fragmented long linear chains into shorter segments and converted branched chains into linear structures. This synergistic effect between MA and enzymatic hydrolysis resulted in retrograded starch with enhanced short-range molecular order, increased crystallinity, and significantly high RS content.

Starch retrogradation is closely related to the ordered structure of starch molecules and the gel dehydration and shrinkage process, all of which are influenced by the moisture state. LF-NMR analysis was applied to measure the transverse relaxation times of starch samples for characterizing the distribution and migration of water during retrogradation. The water distribution, transverse relaxation time distribution, and peak areas of different starch samples are shown in Fig. 1d and Table S2. $T_{21/2b}$ (0.01–3.0 ms) and T_{22} (4.0–100 ms) represent tightly bound water and weakly bound water, respectively [43, 44]. Since this study focused on semi-solid starch samples with low moisture content, all water involved in the gelatinization process was tightly bound to the starch chains, and thus free water was not detected [45]. The $T_{21/2b}$ values of the treated starch samples showed a decreasing trend, while the peak areas increased, indicating that the tightly bound water was more strongly associated with the starch molecules after treatment, and the interactions between them were intensified. Compared with other control samples, EMS exhibited the largest reduction in $T_{21/2b}$, indicating that MA combined with enzymatic hydrolysis treatment enhanced the binding strength of tightly bound water to starch molecules. This enhancement could be attributed to the destruction of crystalline regions within the starch and the exposure of additional hydroxyl groups, allowing water molecules to penetrate more easily and form stronger hydrogen bonds.

The primary water component in the system (T_{22}) is located in the amorphous regions of the outer layer of starch granules, which contains starch fragments and colloidal substances. These regions enhance water interaction through dissolution and swelling. After MA combined with enzymatic hydrolysis treatment, the destruction of crystalline regions increased the surface area for water contact. Although the T_{22} value slightly decreased, the peak area increased, indicating that the weakly bound water became more tightly associated with the starch molecules, significantly strengthening their interaction. These changes could be explained by the following factors: (1) The treatment increased the amorphous regions in the starch by breaking crystalline areas, improving water penetration. (2) MA combined with enzymatic hydrolysis treatment exposed more hydroxyl groups on the starch surface, enhancing water binding. (3) The processed short-chain amylose dissolved more easily and interacted more thoroughly with water molecules. These findings demonstrated that MA combined with enzymatic hydrolysis treatment significantly improved the water-binding capacity of starch. This enhanced water association during retrogradation facilitated tighter binding between water and starch molecules, promoting the

formation of RS_3. The results highlighted the superiority of this method in disrupting the original starch structure and increasing RS_3 content compared to other treatments.

The thermal properties of different starch samples were analyzed by DSC, as shown in Fig. 1e and Table S3. T_o, T_p, T_c, and ΔH represent the onset temperature, peak temperature, conclusion temperature, and enthalpy, respectively. This process involves the dissolution of amylopectin and resistant starch double-helical crystalline structures during heating. Notably, as the RS_3 content increasing, the T_o, T_p, T_c, and ΔH also increased. Compared with other control samples, EMS exhibited the most significant increases in these thermal parameters, indicating its distinct thermal properties. The observed differences in thermal characteristics could be attributed to the high amylose content in EMS after MA combined with enzymatic hydrolysis treatment. During gelatinization, starch molecules transformed into a disordered state. Subsequently, during retrogradation, these molecules realigned and interacted to form the ordered RS_3 structures. Since RS_3 is the primary factor influencing thermal properties after heat treatment (due to the degradation of RS_2 during heating), the EMS with the highest RS_3 content showed the greatest increases in T_o, T□, T_C, and ΔH values. These findings suggested that MA combined with enzymatic hydrolysis treatment significantly enhanced the amylose content and RS_3 formation, leading to improved thermal stability and higher energy requirements during gelatinization compared to other treatment methods.

The appearance of the starch samples before and after retrogradation with different treatments is shown in Fig. 2. The results indicated that the treatment methods significantly affected the microstructure of cassava starch. After treatment, the starch granules gradually lost their original round shape and became damaged and deformed. For the starch treated with MA or pullulanase alone (Fig. 2b1 and d1), the shape of the starch granules remained relatively intact, with only slight local damage and indentations on the surface. However, when both MA and pullulanase treatments were applied together (Fig. 2e1 and f1), the shape of the starch granules underwent significant changes, with noticeable angular edges in some areas, and the integrity of the granules was compromised. Furthermore, cassava starch treated by MA and enzymatic hydrolysis not only showed the changes in granule shape but also experienced a transition from a smooth surface to a rougher one. This change was attributed to the mechanical force applied during the MA and enzymatic hydrolysis processes, where repeated collisions between the grinding balls and the powder deformed and fractured the granules. Additionally, the action of pullulanase further eroded the starch surface. Combined with the XRD analysis, this structural damage might lead to the disruption of the dense crystalline structure on the outer layer of the starch, thus affecting its physicochemical properties.

The retrograded starch samples with low RS_3 content, such as S, ES + M, and MS (Fig. 2a2, c2, and d2), exhibited a relatively loose structure, with clear fracture stripes and sharp edges visible on the cross-section, accompanied by loose starch layers. This might be due to the weaker intermolecular forces between the starch chains, which allowed water to distribute within the structure. During the drying process, the exudation of water resulted in this structure. On the other hand, the samples with high RS_3

content, such as ES, MS + E, and EMS (Fig. 2b2, e2, and f2), displayed a denser structure with less noticeable and fewer angular edges. This could be due that during retrogradation, water continuously migrated and exuded, strengthening the hydrogen bonds between starch chains and leading to a more compact and solid structure, which appeared smooth and tightly packed. In general, as the RS_3 content increased, the retrogradation of starch deepened, resulting in closer binding between the starch chains and a smoother surface [46].

Effects of different factors on RS content in EMS

The effects of various factors on the RS_3 content in EMS are shown in Fig. 3. Figure 3a illustrates the influence of MA temperature on the RS_3 content. The RS_3 content increased gradually with the MA temperature increasing, suggesting that high temperature facilitated RS_3 formation. This was likely due to enhanced pullulanase activity at elevated temperature, leading to high yields of amylose and subsequently increasing RS_3 content after retrogradation, with a peak value at 50°C. However, further increasing the temperature exceeded the optimal range for pullulanase activity, suppressing enzyme efficiency. As a result, the amount of amylose generated from debranched amylopectin decreased, causing a reduction in RS_3 content. The above results indicated that the optimal MA temperature was 50°C.

Figure 3b demonstrates the effect of MA time on the RS_3 content. The RS_3 content increased progressively as prolonging MA time, with a peak value at 6 h. This was attributed to the amylopectin was continuously broken into amylose by mechanical force during the MA process. Additionally, MA disrupted the original crystalline structure of cassava starch, allowing pullulanase to penetrate more easily, thereby improving the enzymatic efficiency and producing more amylose. MA also enhanced the molecular motion and interactions, forming strong hydrogen bonds through abundant hydroxyl groups, which promoted the formation of RS_3. However, when the time exceeded 6 h, RS_3 content declined significantly, indicating that excessive mechanical force overly fragmented the molecular chains. The resulting short chains inhibited starch retrogradation, which was detrimental to RS_3 formation [36].

Figure 3c illustrates the effect of starch concentration on the RS_3 content. The RS_3 content increased progressively with the starch concentration increasing, reaching a maximum value at a concentration of 20 wt%. At low starch concentrations, the gap between starch particles and grinding balls in the milling device was too large, which reduced the efficiency of mechanical forces in breaking down starch molecules and disrupting crystalline regions, resulting in a low amylose content. As the starch concentration increased, the mechanical forces became more effective, and the MA combined with enzymatic treatment cleaved more amylopectin into amylose, thereby enhancing RS_3 content. However, when the starch concentration exceeded 20 wt%, the high molecular density restricted effective interaction between pullulanase and starch molecules, reducing enzymatic hydrolysis efficiency, lowering amylose production, and subsequently decreasing RS_3 formation.

Figure 3d shows the effect of pullulanase dosage on the RS_3 content. The RS_3 content increased with the pullulanase dosage increasing. This was because pullulanase cleaved α-1,6-glycosidic bonds at branch points in amylopectin, promoting the conversion of amylopectin to amylose and further increasing the RS_3 content. However, when the pullulanase dosage exceeded 20 u g^{-1}, the RS_3 content plateaued. At this point, the enzyme was sufficient to react with the starch, and any additional pullulanase did not contribute further to the hydrolysis of cassava starch, resulting in no significant increase in RS_3 content. In consequence, the optimal conditions for preparing EMS were identified as starch concentration of 20 wt%, pullulanase dosage of 20 u g^{-1}, MA temperature of 50°C, and MA time of 6 h. Under these conditions, the RS content in EMS was 23.6%.

Moreover, Table S1 presents the comparison of the effects of different treatment methods on the RS_3 content in starch. It was observed that the combination of MA treatment followed by freeze-thaw treatment increased the RS_3 content in high-amylose maize starch from 36.7% to 51.4% [27]. MA treatment alone increased the RS_3 content in cassava starch from 3.8% to 13.5% [37]. After treatment with pullulanase, the RS_3 content in waxy maize starch increased from 13.0% to 19.0% [38]. For sweet potato starch, autoclaving and pullulanase treatment increased the RS_3 content from 1.4% to 15.9%. Microwave–toughening treatment led to an increase in RS_3 content in potato starch from 11.5% to 27.1% [39, 40]. In this study, MA combined with enzymatic hydrolysis treatment increased the RS_3 content in cassava starch from 5.8% to 23.6%, with an increase of 17.8%, which was the highest RS_3 value. These results indicated that MA combined with enzymatic hydrolysis treatment was more effective in enhancing the RS_3 in starch than single treatment methods, as well as other treatment approaches.

Formation mechanism of RS_3

Based on the above results, a mechanism for the formation of RS_3 in EMS was proposed, as illustrated in Fig. 4. Cassava starch contains a higher proportion of branched amylopectin molecules and a lower proportion of amylose molecules. During MA, the collisions and compressive forces led to the breakage of molecular chains, shortening the starch molecules and disrupting the crystalline structure of starch. This enhanced the mobility of the starch molecules and increased the number of free –OH groups, allowing pullulanase to penetrate the starch granules and cleave the α-1,6-glycosidic bonds of amylopectin, increasing the amylose content. Meanwhile, after enzymatic hydrolysis treatment, the starch granules lost their original shape, and refrigerated storage further accelerated the interaction between amylose molecules, promoting the formation of hydrogen bonds between –OH groups. This process accelerated the formation of the double helix structure and recrystallization regions of RS_3.

GI analysis of biscuits

Figure 5a shows the effect of different treatments on the *in vitro* starch digestibility of biscuits. The results indicated that the starch hydrolysis rate of all samples gradually increased with the digestion

time increasing, reaching the highest rate at 30 min, after which the digestion rate plateaued at 90 min. Specifically, the biscuits made from S exhibited the highest starch digestibility, while those made from EMS showed the lowest digestibility. This could be attributed to the high RS content in EMS, where the dense crystalline structure of the starch slowed down the action of α-amylase [47]. Figure 5b shows the expected GI value of the biscuits. Compared with other control samples, the EMS biscuits had the lowest GI value (53.3), indicating that the MA combined with enzymatic hydrolysis treatment reduced the GI value of biscuits, which was attributed to the high RS content in EMS. The GI value of EMS biscuits was < 55, classifying them as low-GI foods. Moreover, Table S3 shows the comparation of the RS contents and GI values of reported RS foods from various studies. Compared with other reported samples, the EMS sample in this study demonstrated a competitive advantage in both RS content and GI value. This suggested that resistant cassava starch prepared by MA combined with enzymatic hydrolysis method could be used as a functional ingredient in low-GI foods, which might help prevent certain degenerative diseases, such as obesity, diabetes, and cancer.

Sensory evaluation of biscuits

Previous study has found that cassava starch with a damage level of 15.37% (DSC) was suitable for cookie preparation [37]. The photographs and overall sensory scores of the biscuits made from DSC and the samples prepared in this study are shown in Fig. 6b, while Fig. 6a displays the radar chart for all biscuits. The sensory evaluation score of the EMS biscuits was 43.0, slightly lower than that of the DSC biscuits (43.9). Compared to the DSC biscuits, the EMS biscuits showed superior internal structure crispness, though the internal texture was slightly better in the DSC biscuits. There were no significant differences in appearance, color, or taste between the two types. Overall, the sensory quality of the EMS biscuits was within an acceptable range. Compared to all other samples, the EMS biscuits exhibited slight gaps in internal structure due to the presence of a high content of RS. However, this did not result in a lower sensory appeal but rather contributed to enhanced crispness. This indicated that the application of EMS in food development was feasible and held promise.

Conclusion

This study presented a novel method of MA combined with enzymatic hydrolysis for preparing cassava resistant starch with a RS_3 content of 23.6%. The MA combined with enzymatic hydrolysis treatment effectively disrupted the starch crystalline regions, accelerated the enzymatic hydrolysis efficiency of pullulanase, and generated more short amylose chains suitable for retrogradation, leading to an increased RS_3 content in the cassava starch. The EMS exhibited increased crystallinity and $IR_{1047/1022}$ of 26.69% and 1.039, respectively. The relaxation times of water ($T_{21/b}$ and T_{22}) decreased to 0.69 and 18.77 ms, while the gelatinization temperature range expanded to 62.05–74.68 °C. These findings indicated that the MA combined with enzymatic hydrolysis treatment could promote the generation of a denser crystalline structure, resulting in tighter binding between water and starch molecules and a higher gelatinization temperature, all of which were favorable for the formation of RS_3. The biscuits made from EMS demonstrated favorable sensory properties, and the GI value was below 55, meeting the criteria of

low-GI foods. This work provides a new strategy for increasing the RS content in high-amylopectin starch to produce functional low-GI foods.

Declarations

Funding Declaration

This work was supported by the National Natural Science Foundation of China (No. 22268005) and Guangxi Science and Technology Plan Project, China (Grant No. AB23075132).

Author contributions

Zexiong Huang and Tianyi Guo: Methodology, Validation, Formal analysis, Investigation, Writing – review & editing. Xiaohua Huang and Chen Liang: Investigation, Formal analysis. Mingyu Chen and Yanjuan Zhang: Investigation. Zuqiang Huang and Huayu Hu: Supervision. Tao Gan: Methodology, Supervision, Writing – review & editing, Resources.

Data availability statement

The data that support the findings of this study are available from the corresponding author upon reasonable request

Competing interests

The authors declare that they have no known competing financial interests or personal relationships that could have appeared to influence the work reported in this paper.

Supporting information

Supporting information may be found in the online version of this article

References

1. D.J. Jenkins, T.M. Wolever, R.H. Taylor, H. Barker, H. Fielden, J.M. Baldwin, A.C. Bowling, H.C. Newman, A.L. Jenkins, D.V. Goff, Glycemic index of foods: a physiological basis for carbohydrate exchange. *American Journal of Clinical Nutrition* **1981** *3* (34) 362-366. DOI: 10.1093/ajcn/34.3.362.
2. A. Bojarczuk, P. Kęszycka, K. Marszałek, D. Gajewska, The Effect of Cooking and Cooling Chickpea Pasta on Resistant Starch Content, Glycemic Response, and Glycemic Index in Healthy Adults. *Metabolites* **2024** *11* (14) 585. DOI: 10.3390/metabo14110585.
3. D.J. Jenkins, M.J. Thorne, K. Camelon, A. Jenkins, A.V. Rao, R.H. Taylor, L.U. Thompson, J. Kalmusky, R. Reichert, T. Francis, Effect of processing on digestibility and the blood glucose response: a study of lentils. *The American journal of clinical nutrition* **1982** *6* (36) 1093-101. DOI: 10.1093/ajcn/36.6.1093.

4. I. Pasqualoni, R. Tolve, B. Simonato, F. Bianchi, The Impact of Selected Ingredients on the Predicted Glycemic Index and Technological Properties of Bread. *Foods (Basel, Switzerland)* **2024** *16* (13) DOI: 10.3390/foods13162488.
5. M.K. Lal, B. Singh, S. Sharma, M.P. Singh, A. Kumar, Glycemic index of starchy crops and factors affecting its digestibility: A review. *Trends in Food Science & Technology* **2021** (111) 741-755. DOI: 10.1016/j.tifs.2021.02.067.
6. N. Ratnaningsih, Suparmo, E. Harmayani, Y. Marsono, Physicochemical properties, in vitro starch digestibility, and estimated glycemic index of resistant starch from cowpea (Vigna unguiculata) starch by autoclaving-cooling cycles. *International Journal of Biological Macromolecules* **2020** (142) 191-200. DOI: 10.1016/j.ijbiomac.2019.09.092.
7. J. Wen, M. Li, J. Hu, H. Tan, S. Nie, Resistant starches and gut microbiota. *Food Chemistry* **2022** (387) 132895. DOI: 10.1016/j.foodchem.2022.132895.
8. P.A. Dobranowski, A. Stintzi, Resistant starch, microbiome, and precision modulation. *Gut microbes* **2021** *1* (13) 1926842. DOI: 10.1080/19490976.2021.1926842.
9. F. Jiang, C. Du, W. Jiang, L. Wang, S. Du, The preparation, formation, fermentability, and applications of resistant starch. *International Journal of Biological Macromolecules* **2020** (150) 1155-1161. DOI: 10.1016/j.ijbiomac.2019.10.124.
10. Z. Wang, S. Wang, Q. Xu, Q. Kong, F. Li, L. Lu, Y. Xu, Y. Wei, Synthesis and Functions of Resistant Starch. *Advances in Nutrition* **2023** *5* (14) 1131-1144. DOI: 10.1016/j.advnut.2023.06.001.
11. E. Agama-Acevedo, G. Pacheco-Vargas, L.A. Bello-Pérez, J. Alvarez-Ramirez, Effect of drying method and hydrothermal treatment of pregelatinized Hylon VII starch on resistant starch content. *Food Hydrocolloids* **2018** (77) 817-824. DOI: 10.1016/j.foodhyd.2017.11.025.
12. Z. Huang, J. LU, X. LI, Z. TONG, Effect of mechanical activation on physico-chemical properties and structure of cassava starch. *Carbohydrate Polymers* **2007** *1* (68) 128-135. DOI: 10.1016/j.carbpol.2006.07.017.
13. P. Lertwanawatana, R.A. Frazier, K. Niranjan, High pressure intensification of cassava resistant starch (RS3) yields. *Food Chemistry* **2015** (181) 85-93. DOI: 10.1016/j.foodchem.2015.02.005.
14. T.M. Masatcioglu, Z. Sumer, H. Koksel, An innovative approach for significantly increasing enzyme resistant starch type 3 content in high amylose starches by using extrusion cooking. *Journal of Cereal Science* **2017** (74) 95-102. DOI: 10.1016/j.jcs.2017.01.015.
15. R. Wang, P. Rui, T. Wang, W. Feng, Z. Chen, X. Luo, H. Zhang, Resistant starch formation mechanism of amylosucrase-modified starches with crystalline structure enhanced by hydrothermal treatment. *Food Chemistry* **2023** (414) 135703. DOI: 10.1016/j.foodchem.2023.135703.
16. C. Zhang, M. Qiu, T. Wang, L. Luo, W. Xu, J. Wu, F. Zhao, K. Liu, Y. Zhang, X. Wang, Preparation, structure characterization, and specific gut microbiota properties related to anti-hyperlipidemic action of type 3 resistant starch from Canna edulis. *Food Chemistry* **2021** (351) 129340. DOI: 10.1016/j.foodchem.2021.129340.

17. M. Kapelko, T. Zięba, A. Golachowski, A. Gryszkin, Effect of the production method on the properties of RS3/RS4 type resistant starch. Part 1: Properties of retrograded starch (RS3) produced under various conditions and its susceptibility to acetylation. *Food Chemistry* **2012** *3* (135) 1494-1504. DOI: 10.1016/j.foodchem.2012.06.030.
18. H. Si, F. Xie, R. Yang, W. Gu, S. Wu, J. Zhang, Y. Zhang, Y. Qiao, Recent developments in enzymatic preparation, physicochemical properties, bioactivity, and application of resistant starch type III from staple food grains. *International Journal of Biological Macromolecules* **2024** (279) 135521. DOI: 10.1016/j.ijbiomac.2024.135521.
19. A.A. Karim, M.H. Norziah, C.C. Seow, Methods for the study of starch retrogradation. *Food Chemistry* **2000** *1* (71) 9-36. DOI: 10.1016/S0308-8146(00)00130-8.
20. Q. Liu, J. Shi, Z. Jin, A. Jiao, Development and characterization of resistant starch produced by an extrusion–debranching strategy with a high starch concentration. *Food Hydrocolloids* **2023** (136) 108276. DOI: 10.1016/j.foodhyd.2022.108276.
21. H.X.N. Doan, Y. Song, S. Lee, B.H. Lee, S.H. Yoo, Characterization of rice starch gels reinforced with enzymatically-produced resistant starch. *Food Hydrocolloids* **2019** *JUN.* (91) 76-82. DOI: 10.1016/j.foodhyd.2019.01.014.
22. H. Demirkesen-Bicak, Z. Tacer-Caba, D. Nilufer-Erdil, Pullulanase treatments to increase resistant starch content of black chickpea (Cicer arietinum L.) starch and the effects on starch properties. *International Journal of Biological Macromolecules* **2018** (111) 505-513. DOI: 10.1016/j.ijbiomac.2018.01.026.
23. P. Manimegalai, R. Parimalavalli, Effect of pullulanase debranching on the yield of retrograded pearl millet starch and its intrinsic qualities. *Food Measure* **2023** *3* (17) 2566-2575. DOI: 10.1007/s11694-022-01779-3.
24. G.N. Barrera, G.T. Pérez, P.D. Ribotta, A.E. León, Influence of damaged starch on cookie and bread-making quality. *Eur Food Res Technol* **2007** *1* (225) 1-7. DOI: 10.1007/s00217-006-0374-1.
25. Z. Fu, L. Che, D. Li, L. Wang, B. Adhikari, Effect of partially gelatinized corn starch on the rheological properties of wheat dough. *LWT - Food Science and Technology* **2016** (66) 324-331. DOI: 10.1016/j.lwt.2015.10.052.
26. Z. Huang, X. Xie, Y. Chen, J. Lu, Z. Tong, Ball-milling treatment effect on physicochemical properties and features for cassava and maize starches. *Comptes Rendus Chimie* **2008** *1-2* (11) 73-79. DOI: 10.1016/j.crci.2007.04.008.
27. W. Li, Z. Zhou, S. Fan, X. Cai, J. Chen, Y. Zhang, Z. Huang, H. Hu, J. Liang, Formation of type 3 resistant starch from mechanical activation-damaged high-amylose maize starch by a high-solid method. *Food Chemistry* **2021** (363) 130344. DOI: 10.1016/j.foodchem.2021.130344.
28. Q. Wang, L. Li, X. Zheng, A review of milling damaged starch: Generation, measurement, functionality and its effect on starch-based food systems. *Food Chemistry* **2020** (315) 126267. DOI: 10.1016/j.foodchem.2020.126267.

29. Y. Zhang, J. Wang, P. Yang, Convenient synthesis of Ag nanowires with tunable length and morphology. *Materials Research Bulletin* **2013** *2* (48) 461-468. DOI: 10.1016/j.materresbull.2012.11.011.
30. R. Liu, Y. Zhang, H. Hu, T. Gan, Z. Huang, Retrogradation behavior of starch dough prepared from damaged cassava starch and its application in functional gluten-free noodles. *International Journal of Biological Macromolecules* **2023** (236) 123996. DOI: 10.1016/j.ijbiomac.2023.123996.
31. O.F. Osundahunsi, K.T. Seidu, R. Mueller, Effect of presence of sulphurdioxide on acetylation and sorption isotherm of acetylated starches from cultivars of cassava. *Food Chemistry* **2014** (151) 168-174. DOI: 10.1016/j.foodchem.2013.11.020.
32. K.S. Tumwesigye, J.C. Oliveira, M.J.S. Gallagher, Integrated sustainable process design framework for cassava biobased packaging materials: Critical review of current challenges, emerging trends and prospects. *Trends in Food Science & Technology* **2016** (56) 103-114. DOI: 10.1016/j.tifs.2016.08.001.
33. F. Zhu, Composition, structure, physicochemical properties, and modifications of cassava starch. *Carbohydrate Polymers* **2015** (122) 456-480. DOI: 10.1016/j.carbpol.2014.10.063.
34. I. Goni, A. GarciaAlonso, F. SauraCalixto, A starch hydrolysis procedure to estimate glycemic index. *Nutrition Research* **1997** *3* (17) 427-437. DOI: DOI 10.1016/S0271-5317(97)00010-9.
35. J. Kampa, S.P. Bull, A. Signorello, R.A. Frazier, J. Rodriguez-Garcia, Saturated fat replacement in short dough biscuits with HPMC and lecithin stabilised nanoemulsions. *npj Science of Food* **2023** *1* (7) 26-26. DOI: 10.1038/s41538-023-00202-5.
36. Tuangporn, Tukomane, Saiyavit, Varavinit, Classification of Rice Starch Amylose Content from Rheological Changes of Starch Paste after Cold Recrystallization. *Starch* **2008** DOI: 10.1002/star.200700672.
37. R. Liu, W. Sun, Y. Zhang, Z. Huang, H. Hu, M. Zhao, Preparation of starch dough using damaged cassava starch induced by mechanical activation to develop staple foods: Application in crackers. *Food Chemistry* **2019** (271) 284-290. DOI: 10.1016/j.foodchem.2018.07.202.
38. W. Liu, Y. Hong, Z. Gu, L. Cheng, Z. Li, C. Li, In structure and in-vitro digestibility of waxy corn starch debranched by pullulanase. *Food Hydrocolloids* **2016** *JUN.* (67) 104-110. DOI: 10.1016/j.foodhyd.2016.12.036.
39. H. Sun, J. Fan, Z. Tian, L. Ma, Y. Meng, Z. Yang, X. Zeng, X. Liu, L. Kang, X. Nan, Effects of treatment methods on the formation of resistant starch in purple sweet potato. *Food Chemistry* **2022** (367) 130580. DOI: 10.1016/j.foodchem.2021.130580.
40. Y. Li, T. Xu, J. Xiao, A. Zong, B. Qiu, M. Jia, L. Liu, W. Liu, Efficacy of potato resistant starch prepared by microwave–toughening treatment. *Carbohydrate Polymers* **2018** (192) 299-307. DOI: 10.1016/j.carbpol.2018.03.076.
41. J.J.G. van Soest, H. Tournois, D. de Wit, J.F.G. Vliegenthart, Short-range structure in (partially) crystalline potato starch determined with attenuated total reflectance Fourier-transform IR spectroscopy. **1995** (279) 201-214. DOI: 10.1016/0008-6215(95)00270-7.

42. Z. Ma, J.I. Boye, Research advances on structural characterization of resistant starch and its structure-physiological function relationship: A review. *Critical reviews in food science and nutrition* **2018** *7* (58) 1059-1083. DOI: 10.1080/10408398.2016.1230537.
43. H.C. Bertram, S. Donstrup, A.H. Karlsson, H.J. Andersen, Continuous distribution analysis of T(2) relaxation in meat-an approach in the determination of water-holding capacity. *Meat science* **2002** *3* (60) 279-85. DOI: 10.1016/s0309-1740(01)00134-6.
44. H.R. Tang, J. Godward, B. Hills, The distribution of water in native starch granules—a multinuclear NMR study. *Carbohydrate Polymers* **2000** *4* (43) 375-387. DOI: 10.1016/S0144-8617(00)00183-1.
45. L. Chen, Y. Tian, Q. Tong, Z. Zhang, Z. Jin, Effect of pullulan on the water distribution, microstructure and textural properties of rice starch gels during cold storage. *Food Chemistry* **2017** (214) 702-709. DOI: 10.1016/j.foodchem.2016.07.122.
46. X. Liu, L. Qiao, Y. Kong, H. Wang, B. Yang, Characterization of the starch molecular structure of wheat varying in the content of resistant starch. *Food Chemistry: X* **2024** (21) 101103. DOI: 10.1016/j.fochx.2023.101103.
47. P. Van Hung, H.T. Chau, N.T.L. Phi, In vitro digestibility and in vivo glucose response of native and physically modified rice starches varying amylose contents. *Food Chemistry* **2016** (191) 74-80. DOI: 10.1016/j.foodchem.2015.02.118.

Figures

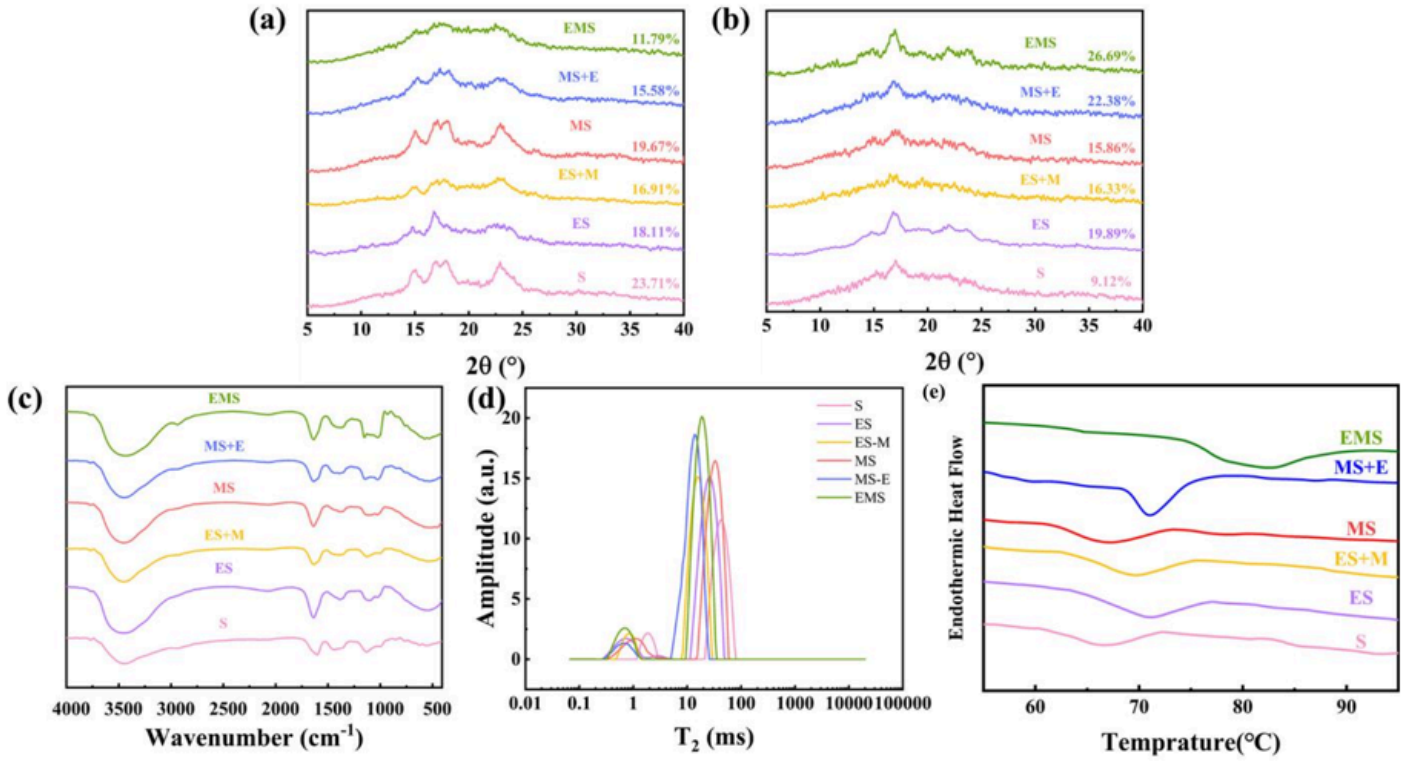

Figure 1

(a) XRD patterns of the native starch samples with different treatments. (b) XRD patterns of the retrograde starch samples with different treatments. (c) FT-IR spectra and (d) transverse relaxation time of water distribution in starch-water system of the starch samples with different treatments. (e) DSC curves of different treatment conditions.

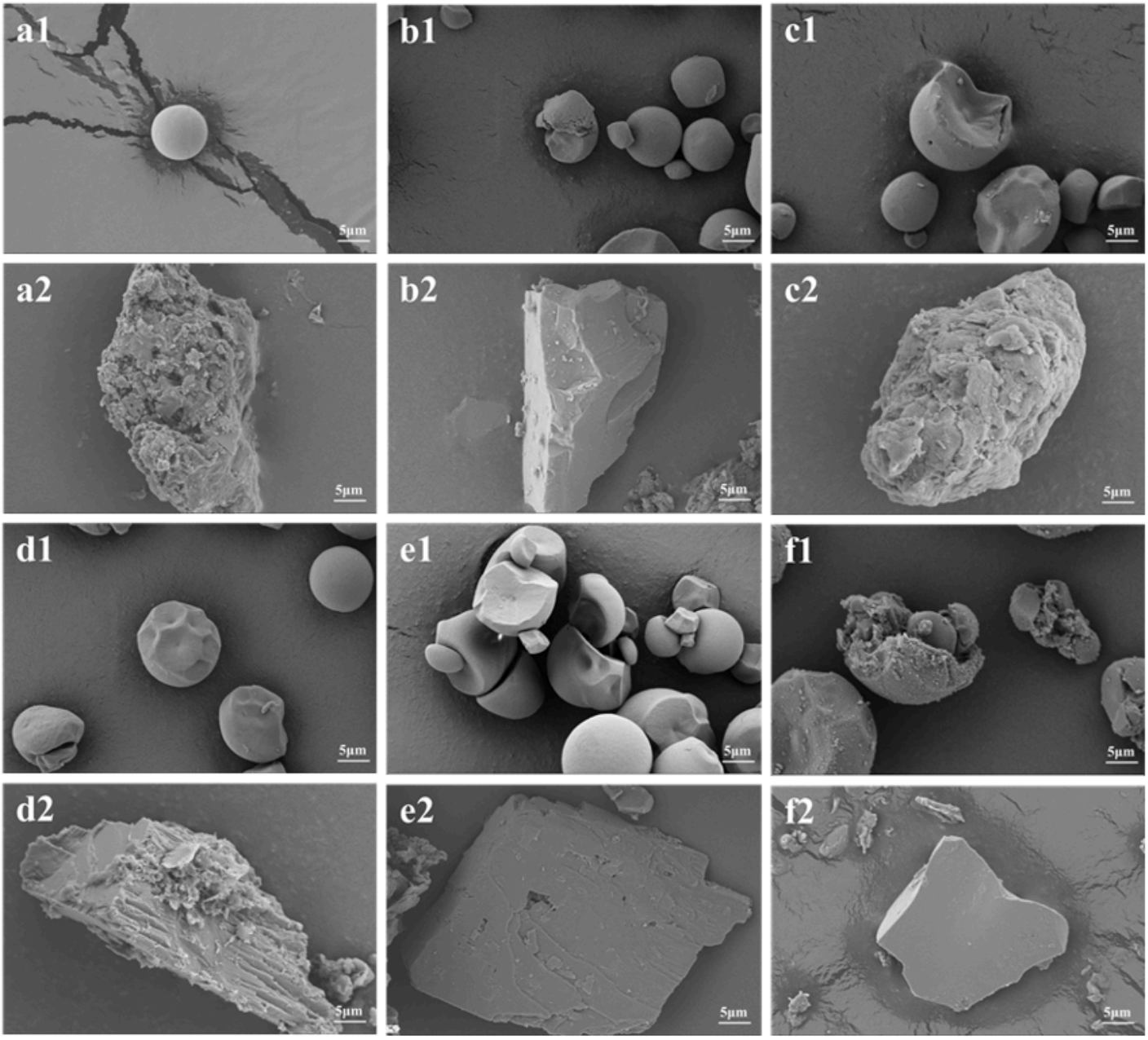

Figure 2

SEM images of (a) S, (b) ES, (c) ES+M, (d) MS, (e) MS+E, and (f) EMS (1 and 2 represent native starch and retrograded starch samples prepared by different treatments).

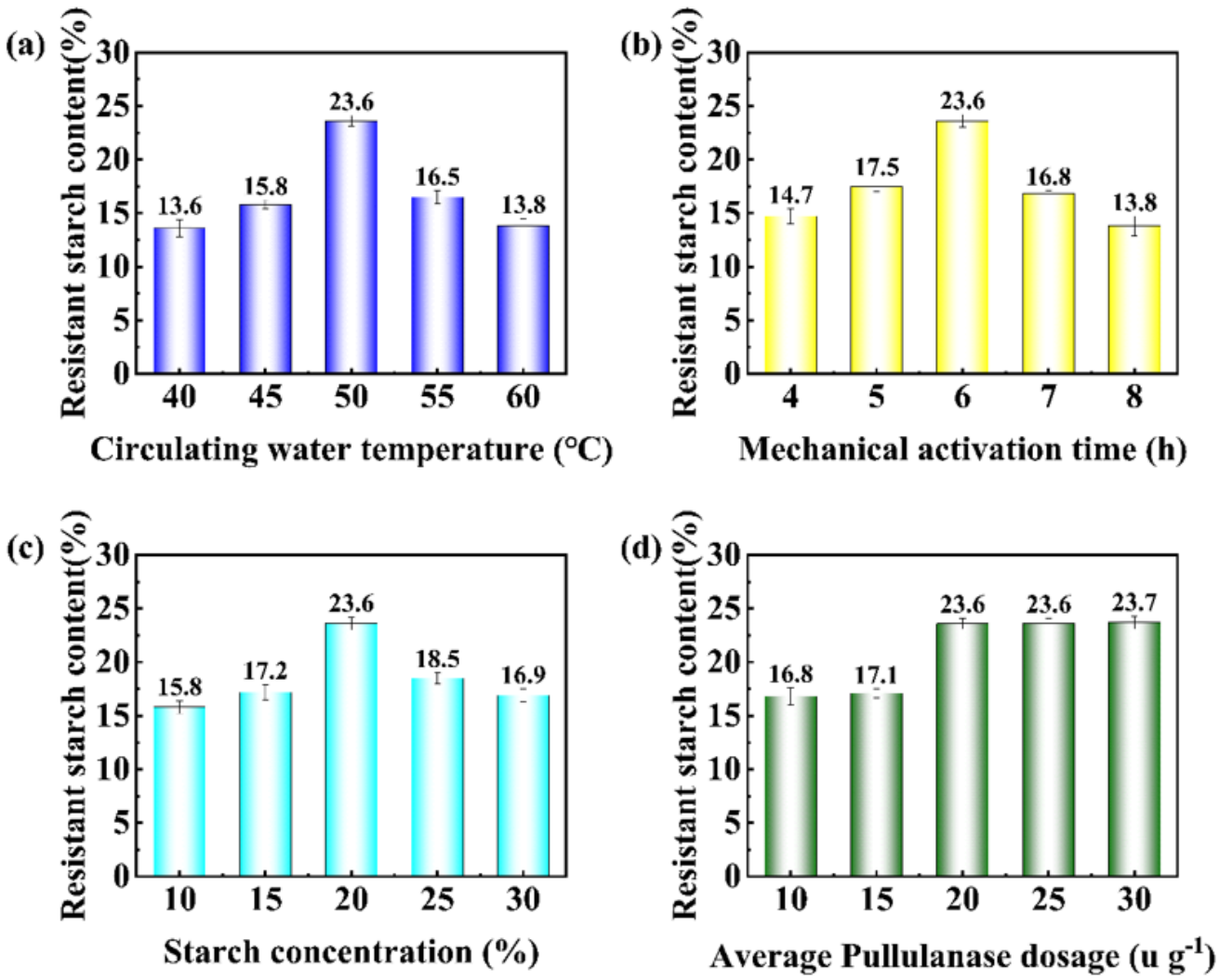

Figure 3

Effects of (a) MA temperature, (b) MA time, (c) starch concentration, and (d) average pulluanase dosage on RS_3 content in EMS.

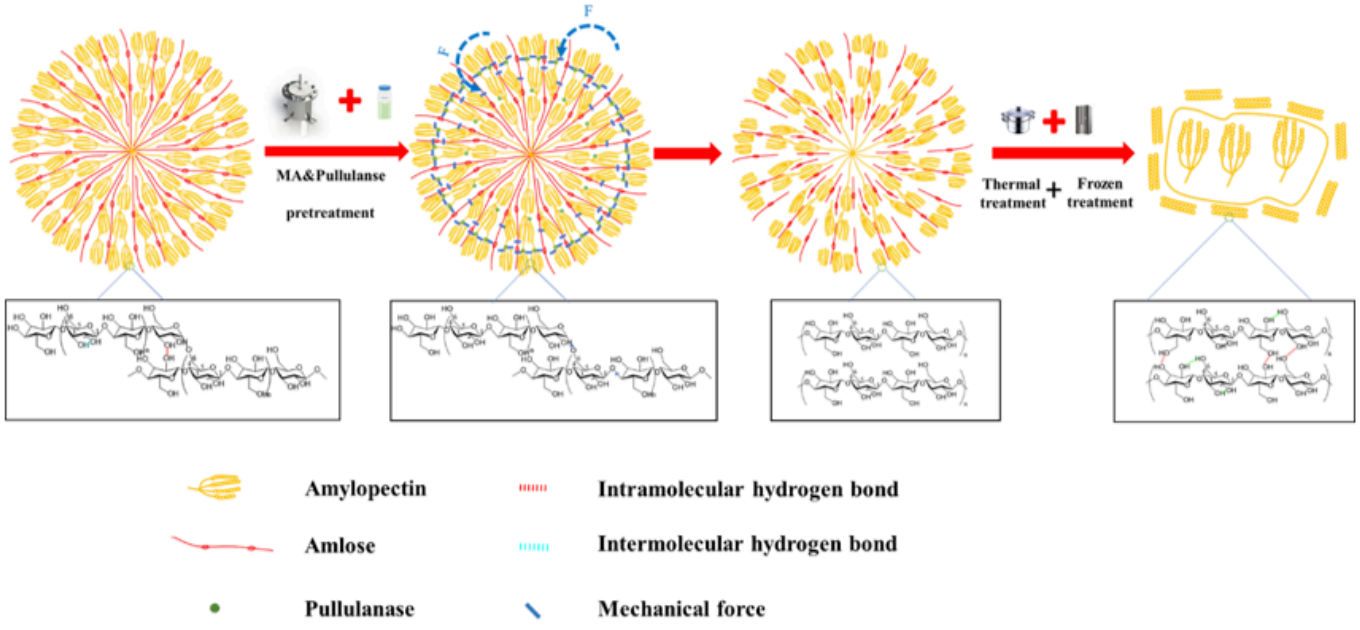

Figure 4

The formation mechanism of RS_3 in EMS.

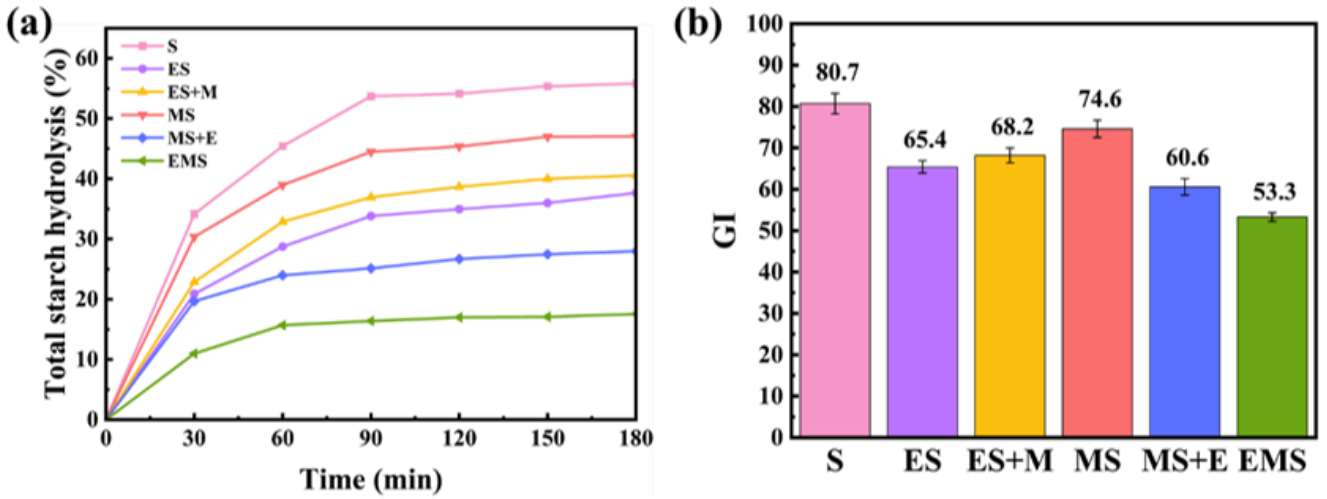

Figure 5

(a) *In vitro* digestion grams and (b) GI values of the biscuits made from different starch samples.

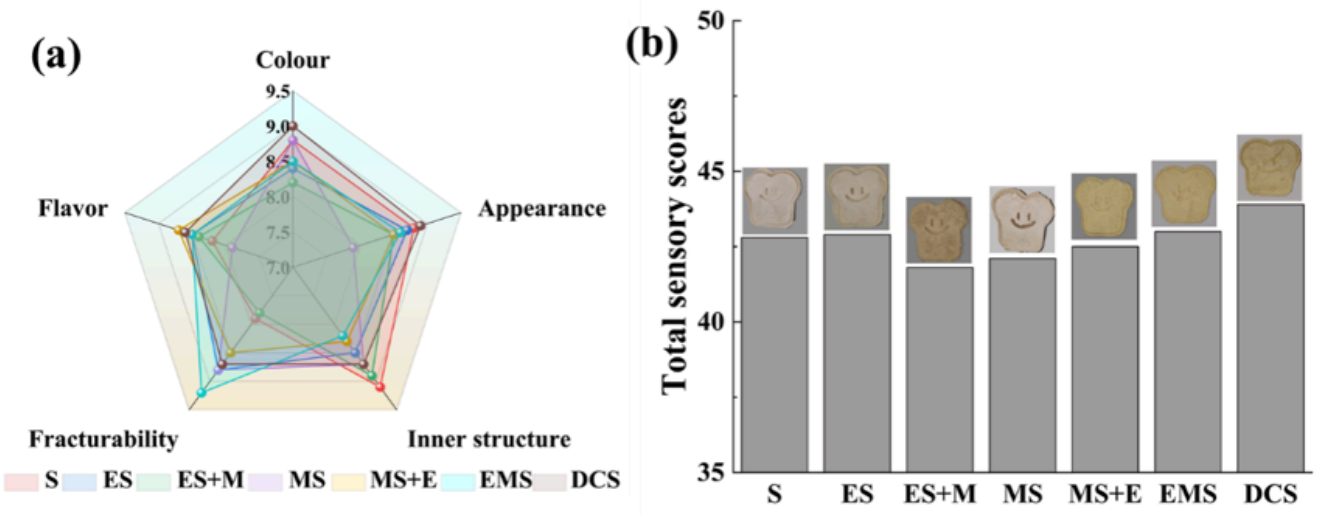

Figure 6

(a) Radar chart of sensory scores and (b) bar chart on sensory assessment for total point of the biscuits made different samples.

Supplementary Files

This is a list of supplementary files associated with this preprint. Click to download.

- SupplementaryMaterial1.docx